Preprints of the 21st IFAC World Congress (Virtual)
Berlin, Germany, July 12-17, 2020

Adaptive Model Predictive Control of Combustion in Flex-Fuel Heavy Duty Compression-Ignition Engine ⋆

Xiufei Li * **Per Tunestål** * **Rolf Johansson** **

* *Department of Energy Sciences, Lund University, Lund, Sweden (e-mail: xiufei.li@energy.lth.se, per.tunestal@energy.lth.se)*
** *Department of Automatic Control, Lund University, Lund, Sweden (e-mail: rolf.johansson@control.lth.se)*

Abstract: Flex-fuel engines can operate on different fuels, from fossil fuel to renewable fuel and their mixture. With the assumption that fuel species is unknown in advance, the mutative fuel properties give rise to an interesting control problem. Since the combustion phasing and ignition delay in the combustion process are intimately coupled, the fuel injection system and air system need to be combined for performance. In this work, an adaptive Model Predictive Control (MPC) approach is proposed to control the combustion process in a multi-cylinder heavy duty compression-ignition (CI) engine. MPC is a suitable design for this multiple inputs/outputs system with actuator constraints, and adaptivity is the solvent for the unknown mutative fuel properties. The combustion timing and ignition delay are extracted from cooled in-cylinder pressure sensors and simultaneously controlled by manipulating injection timings, the intake oxygen concentration, and intake pressure using an exhaust-gas recirculation (EGR) system and a variable-geometry turbocharger (VGT). Diesel, gasoline/n-heptane mixture, and ethanol/n-heptane mixture are used in the experiments. The method is validated in fuel transitions from diesel to gasoline mixture and from gasoline mixture to ethanol mixture.

Keywords: Flex-Fuel Engine, Adaptive MPC

1. INTRODUCTION

The flex-fuel engine can operate on different fuels and their mixture. Nowadays, flex-fuel engine mainly refer to spark-ignition (SI) engine operating on a blend of ethanol and gasoline in any volumetric concentration of up to 85% ethanol (93% in Brazil) (Ahn et al., 2010). However, this definition of the flex-fuel engine is narrow. Compression-ignition (CI) engine, operating normally on diesel and biodiesel, can also serve as the flex-fuel engine.

Extensive studies have been carried on the combustion mode of CI engine with gasoline. Well-known modes include homogeneous charge compression ignition (HCCI) (Thring, 1989), partially premixed combustion (PPC) (Manente et al., 2009), and reactivity controlled compression ignition (RCCI) (Reitz and Duraisamy, 2015). Ethanol also has been proven to be a possible fuel for the CI engine. Mack et al. (2009) showed the use of wet ethanol in HCCI mode. Not limited to the blend of gasoline and ethanol, the CI engine can operate on diesel, biodiesel, gasoline, and ethanol, and provide a more flexible range of fuel choice.

⋆ The author would like to acknowledge the Competence Centre for the Combustion Processes, KCFP, and the Swedish Energy Agency for the financial support, Scania for supplying the experimental engine. The Chinese Scholarship Council is also thanked for the sponsorship of living expenses during the authors research. Rolf Johansson is a member of the eLLIIT Excellence Center at Lund University.

The flex-fuel CI engine brings up new control challenges. When operating only on gasoline and ethanol, flex-fuel SI engine primitive task is the detection of ethanol concentration in fuel. This can be done by using ethanol sensor, or by exploiting the difference in stoichiometric air-to-fuel ratio or the latent heat of vaporization between ethanol and gasoline (Ahn et al., 2010). Once the volumetric ethanol concentration is determined, the fuel properties can be assumed all known and further control algorithms are applied. However, the flex-fuel CI engine is expected to operate on more than two specific fuels. Unlike the flex-fuel SI engine, the flex-fuel CI engine doesn't know the fuel species in advance. Consequently, the control method based on detecting specific fuel concentration and thus getting the exact fuel properties information will not work.

This article proposed an adaptive model predictive control approach to control the flex-fuel CI engine combustion process with mutative, unknown fuel contents. The adaptivity is necessary to track the varying fuel properties and its influence on the engine. The high variations of renewable fuel characteristics also put demands on controller adaptivity. The desired fuel features were estimated and updated in real-time by Kalman filter. The control targets are the combustion phasing θ_{CA50} and the ignition delay τ. The combustion phasing and ignition delay influence engine efficiency, emission, noise, etc (Heywood, 2018). Since combustion phasing and ignition delay are intimately coupled, the fuel injection system and air system need to be combined. The actuators are injection timings, the

exhaust-gas recirculation (EGR) system, and the variable-geometry turbocharger (VGT), EGR and VGT being used to manipulate the intake oxygen concentration and intake pressure. Model predictive control (MPC) is a suitable design for the multiple input/output system with actuator constraints (Maciejowski, 2002).

MPC has been applied in many areas of engine control. Bengtsson et al. (2006) showed that MPC is a promising control method for an HCCI engine. Ingesson et al. (2015) and Yin et al. (2019) applied MPC to PPC combustion control. Li et al. (2019) combined MPC with the learning method to handle PPC combustion variations.

The remainder of this paper is organized as follows: section 2 introduces system modeling. In Sec. 3, an adaptive MPC design is elucidated. Section 4 is the experimental set-up. Section 5 presents the experimental results and analysis. The conclusions are given in Section 6.

2. SYSTEM MODELLING

2.1 Heat-Release Analysis

The combustion information is extracted from in-cylinder pressure per cycle for each cylinder. This process is model-based signal processing, called heat-release analysis. The control targets, combustion timing θ_{CA50} and ignition delay τ, are derived from the calculated heat-release. Due to the pressure sensor offset, the pressure signal is pegged with respect to the inlet pressure at intake valve closing (IVC). A zero-phase digital filter attenuated high frequency noise in pressure signal.

The heat-release rate is the derivative of cumulative released heat Q_c with respect to the crank angle degree (CAD) θ. The variable $\mathrm{d}Q_c/\mathrm{d}\theta$ was estimated by viewing the combustion chamber content as a single-zone open system. Applying the ideal gas law and the first law of thermodynamics yields:

$$\frac{\mathrm{d}Q_c}{\mathrm{d}\theta} = \frac{\gamma}{\gamma-1}p\frac{\mathrm{d}V}{\mathrm{d}\theta} + \frac{1}{\gamma-1}V\frac{\mathrm{d}p}{\mathrm{d}\theta}. \tag{1}$$

where p is in-cylinder pressure, and V is the cylinder volume; $\gamma = c_p/c_v$ is the ratio of specific heats, depending on the cylinder gas composition and temperature.

The variables p and V are assumed to satisfy the adiabatic relation with a constant C:

$$pV^{\gamma} = C \tag{2}$$

Here γ was estimated by a function of cylinder temperature (Li, 2018):

$$\gamma = \gamma_0 - \frac{T-300}{1000}\gamma_{co} \tag{3}$$

where T is the in-cylinder temperature in Kelvin, γ_0 and γ_{co} are constant parameters with a value of 1.3736 and 0.0813.

When the accumulated heat-release Q_c is computed from (1), the combustion phasing θ_{CA50} and θ_{CA10} are calculated. The variables θ_{CA50} and θ_{CA10} are defined as the crank angle degree after top dead center (CAD ATDC) where 50% and 10% total heat are released; θ_{CA50} is the combustion timing and θ_{CA10} is called the start of combustion.

The ignition delay τ in milliseconds is the time between the start of injection θ_{SOI} and the start of combustion θ_{CA10}. One pilot injection was adopted in this paper for promoting combustion and noise reduction. The start of injection θ_{SOI} refers to the main injection timing. τ being calculated by:

$$\tau = \frac{\theta_{CA10} - \theta_{SOI}}{0.006N_{speed}} \tag{4}$$

where θ_{SOI} is the crank angle degree at the start of the injector current impulse and N_{speed} is the engine speed, with the unit of revolutions per minute, rpm.

2.2 Ignition Delay Model

Heat-release analysis is used to obtain the combustion feedback signal. For control applications, it is necessary to model the θ_{CA50} and τ where θ_{CA50} can be computed using (4):

$$\theta_{CA50} = \theta_{SOI} + 0.006N_{speed}\tau + \theta_{CA10-50} \tag{5}$$

where $\theta_{CA10-50}$ is the crank angle degree between θ_{CA10} and θ_{CA50}. Here assumes that the chosen actuators, injection timing, EGR, and VGT valve opening do not influence $\theta_{CA10-50}$. This assumption will not degrade the controller performance much since the main contribution of θ_{CA50} is from the injection timing θ_{SOI} and ignition delay τ.

The ignition delay τ was estimated using an Arrhenius-type model:

$$\tau = c_1 \exp(c_2/\bar{T})\bar{O}_2^{c_3}\bar{p}^{c_4} \tag{6}$$

where c_1, c_3, and c_4 are fuel dependent empirical parameters. $c_2 = E_a/R$ where E_a is the apparent activation energy and R is the universal gas constant. For simplicity, the E_a/R in general Arrhenius-type model was represented by c_2. $\bar{T}, \bar{O}_2, \bar{p}$ are the mean cylinder temperature, oxygen concentration and pressure between θ_{SOI} and θ_{CA10}. The adiabatic relation (2) is assumed to hold during this period.

For control purposes, the in-cylinder pressure p during θ_{SOI} to θ_{CA10} was estimated as:

$$p = p_{IVC}\left(\frac{V_{IVC}}{V}\right)^{\gamma} \tag{7}$$

where p_{IVC} is the measured intake pressure at IVC, and V_{IVC} is the cylinder volume at IVC.

The in-cylinder temperature T was computed using the intake manifold temperature at IVC, which gives:

$$T = T_{IVC}\frac{pV}{p_{IVC}V_{IVC}} = T_{IVC}\left(\frac{V_{IVC}}{V}\right)^{\gamma-1} \tag{8}$$

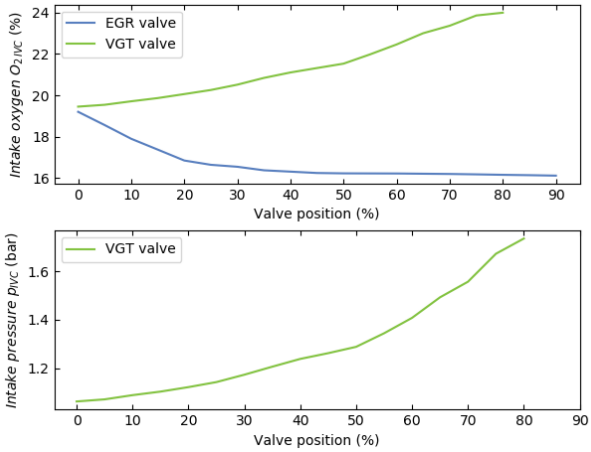

Fig. 1. Intake oxygen $O_{2\,IVC}$ and pressure p_{IVC} as a function EGR and VGT valve positions

where T_{IVC} is the measured intake manifold temperature and at IVC.

The oxygen concentration in cylinder was calculated as follows:

$$O_2 = O_{2\,IVC}\frac{V_{IVC}}{V} \tag{9}$$

where $O_{2\,IVC}$ is the measured intake manifold oxygen concentration in percentage at IVC.

This gives the expression for τ:

$$\tau = c_1 \exp\left(\frac{c_2}{T_{IVC}T_{co}}\right)(O_{2\,IVC}O_{2\,co})^{c_3}(p_{IVC}p_{co})^{c_4} \tag{10}$$

where

$$\begin{aligned} T_{co} &= \frac{\int_{\theta_{SOI}}^{\theta_{SOI}+\tau}\left(\frac{V_{IVC}}{V(\theta)}\right)^{\gamma-1}d\theta}{\int_{\theta_{SOI}}^{\theta_{SOI}+\tau}d\theta} \\ O_{2\,co} &= \frac{\int_{\theta_{SOI}}^{\theta_{SOI}+\tau}\frac{V_{IVC}}{V(\theta)}d\theta}{\int_{\theta_{SOI}}^{\theta_{SOI}+\tau}d\theta} \\ p_{co} &= \frac{\int_{\theta_{SOI}}^{\theta_{SOI}+\tau}\left(\frac{V_{IVC}}{V(\theta)}\right)^{\gamma}d\theta}{\int_{\theta_{SOI}}^{\theta_{SOI}+\tau}d\theta} \end{aligned} \tag{11}$$

The τ in the integration limit is set to last cycle value when calculating.

2.3 Gas System Model

The relationships between the intake oxygen concentration, pressure at IVC and EGR, VGT valves opening were determined by experiments, as shown in Fig. 1.

The EGR valve opening is assumed to have no effect on intake pressure. In the intake manifold, there is one lambda sensor before all cylinders and six pressure sensors for each cylinder. The pressure variations between cylinders are neglected here, i.e., all cylinders use the same intake pressure to VGT valve opening relationship in Fig. 1.

3. ADAPTIVE MPC DESIGN

3.1 Real-Time Parameter Estimation

In our control application, the ignition delay is most prone to be influenced by mutative fuel contents. θ_{CA50} is then affected according to (5). To fulfill the control task, the ignition delay model (10) parameters need to be estimated and updated online with real-time data.

Taking natural logarithm of both sides in (10), we get:

$$\begin{aligned} \ln(\tau) =& \ln(c_1) + \frac{c_2}{T_{IVC}T_{co}} \\ &+ c_3\ln(O_{2\,IVC}O_{2\,co}) + c_4\ln(p_{IVC}p_{co}) \end{aligned} \tag{12}$$

which can be described by the state-space equation:

$$\begin{bmatrix}\ln(c_1^{k+1})\\ c_2^{k+1}\\ c_3^{k+1}\\ c_4^{k+1}\end{bmatrix} = \begin{bmatrix}\ln(c_1^{k})\\ c_2^{k}\\ c_3^{k}\\ c_4^{k}\end{bmatrix} + \boldsymbol{v}^k$$

$$\ln(\tau^k) = \begin{bmatrix}1 & 1/T_{IVC}^kT_{co}^k & \ln(O_{2\,IVC}^kO_{2\,co}^k) & \ln(p_{IVC}^kp_{co}^k)\end{bmatrix}\begin{bmatrix}\ln(c_1^k)\\ c_2^k\\ c_3^k\\ c_4^k\end{bmatrix} + e^k \tag{13}$$

where the k in superscript represents the cycle number; $\boldsymbol{v}^k$ and e^k are the process noise and the observation noise. The classic Kalman filter is then used to estimate the state vector $[\ln(c_1)\ c_2\ c_3\ c_4]^T$. For more details about Kalman filter and its application in real-time identification, please see (Kalman, 1960) and (Johansson, 1993).

Since the fuel contents are varying during this process, the estimated parameters will not converge to certain constant values. Whereas there are no theoretical proofs for the stability of the interconnected MPC, state estimation, and parameter estimation, no significant stability problem appeared in our experiments.

3.2 State-Space Model

The cycle-to-cycle dynamics for each cylinder between control targets θ_{CA50} and τ and control inputs start of injection θ_{SOI}, EGR valve position θ_{EGR} and VGT valve position θ_{VGT} can be written as:

$$\theta_{CA50_i}^{k+1} = \theta_{CA50_i}^{k} + \begin{bmatrix}\frac{\partial\theta_{CA50_i}}{\partial\theta_{SOI_i}} & \frac{\partial\theta_{CA50_i}}{\partial\theta_{EGR}} & \frac{\partial\theta_{CA50_i}}{\partial\theta_{VGT}}\end{bmatrix}\begin{bmatrix}\Delta\theta_{SOI_i}^k\\ \Delta\theta_{EGR}^k\\ \Delta\theta_{VGT}^k\end{bmatrix} \tag{14}$$

$$\tau_i^{k+1} = \tau_i^k + \begin{bmatrix}\frac{\partial\tau_i}{\partial\theta_{SOI_i}} & \frac{\partial\tau_i}{\partial\theta_{EGR}} & \frac{\partial\tau_i}{\partial\theta_{VGT}}\end{bmatrix}\begin{bmatrix}\Delta\theta_{SOI_i}^k\\ \Delta\theta_{EGR}^k\\ \Delta\theta_{VGT}^k\end{bmatrix} \tag{15}$$

where the i in subscript represents the cylinder number, and the k in superscript represents the cycle number. It should be noticed that the injection timing θ_{SOI} can be

adjusted per cylinder, while the θ_{EGR} and θ_{VGT} are same for all cylinders.

The linearized, discrete-time, state-space model of each cylinder used for control is written as:

$$\begin{aligned} \boldsymbol{x}^{k+1} &= \boldsymbol{A}\boldsymbol{x}^k + \boldsymbol{B}\boldsymbol{u}^k \\ \boldsymbol{y}^k &= \boldsymbol{C}\boldsymbol{x}^k \end{aligned} \tag{16}$$

where the state vector $\boldsymbol{x}^k$ at sample index k

$$\boldsymbol{x}^k = \begin{bmatrix} \theta^k_{CA50} \\ \tau^k \\ \theta^k_{SOI} \\ \theta^k_{EGR} \\ \theta^k_{VGT} \end{bmatrix} \tag{17}$$

with input

$$\boldsymbol{u}^k = \begin{bmatrix} \Delta\theta^k_{SOI} \\ \Delta\theta^k_{EGR} \\ \Delta\theta^k_{VGT} \end{bmatrix} \tag{18}$$

and output

$$\boldsymbol{y}^k = \begin{bmatrix} \theta^k_{CA50} \\ \tau^k \end{bmatrix} \tag{19}$$

and state-space matrices

$$\boldsymbol{A} = \boldsymbol{I}_{5\times 5} \tag{20}$$

$$\boldsymbol{B} = \begin{bmatrix} \frac{\partial\theta_{CA50}}{\partial\theta_{SOI}} & \frac{\partial\theta_{CA50}}{\partial\theta_{EGR}} & \frac{\partial\theta_{CA50}}{\partial\theta_{VGT}} \\ \frac{\partial\tau}{\partial\theta_{SOI}} & \frac{\partial\tau}{\partial\theta_{EGR}} & \frac{\partial\tau}{\partial\theta_{VGT}} \\ 1 & 0 & 0 \\ 0 & 1 & 0 \\ 0 & 0 & 1 \end{bmatrix} \tag{21}$$

$$\boldsymbol{C} = \begin{bmatrix} 1 & 0 & 0 & 0 & 0 \\ 0 & 1 & 0 & 0 & 0 \end{bmatrix} \tag{22}$$

The actuators increments were selected as the system inputs. Consequently, θ^k_{SOI}, θ^k_{EGR}, and θ^k_{VGT} are added into the state vector to help set constraints on them.

According to (5), we get:

$$\begin{aligned} \frac{\partial\theta_{CA50}}{\partial\theta_{SOI}} &= 1 \\ \frac{\partial\theta_{CA50}}{\partial\theta_{EGR}} &= 0.006 N_{speed}\frac{\partial\tau}{\partial\theta_{SOI}} \\ \frac{\partial\theta_{CA50}}{\partial\theta_{VGT}} &= 0.006 N_{speed}\frac{\partial\tau}{\partial\theta_{VGT}} \end{aligned} \tag{23}$$

The partial derivatives of τ with respect to θ_{SOI}, $O_{2\,IVC}$, and p_{IVC} are obtained from (10). Although the θ_{SOI} is in the integration limit, its influence on the ignition delay τ is insignificant and neglected for simplicity. We have:

$$\begin{aligned} \frac{\partial\tau}{\partial\theta_{SOI}} &= 0 \\ \frac{\partial\tau}{\partial\theta_{EGR}} &= \frac{\partial\tau}{\partial O_{2\,IVC}}\frac{\partial O_{2\,IVC}}{\partial\theta_{EGR}} \\ \frac{\partial\tau}{\partial\theta_{VGT}} &= \frac{\partial\tau}{\partial O_{2\,IVC}}\frac{\partial O_{2\,IVC}}{\partial\theta_{VGT}} + \frac{\partial\tau}{\partial p_{IVC}}\frac{\partial p_{IVC}}{\partial\theta_{VGT}} \end{aligned} \tag{24}$$

As stated in Sec. 2.3, EGR has no influence on intake pressure, which means $\partial p_{IVC}/\partial\theta_{EGR} = 0$. The value of $\partial O_{2\,IVC}/\partial\theta_{EGR}$, $\partial O_{2\,IVC}/\partial\theta_{VGT}$, and $\partial p_{IVC}/\partial\theta_{VGT}$ are estimated from the slopes in Fig. (1).

3.3 MPC Design

At each time step, the parameters $\ln(c_1)$, c_2, c_3, and c_4 are estimated first with Kalman filter. Then, based on the state-space model (16), a Quadratic Programming (QP) problem will be solved to obtain optimal control inputs:

$$\min_{\boldsymbol{u}} \left(\sum_{k=1}^{H_p} \left\| \boldsymbol{y}^k - \boldsymbol{r} \right\|^2_{\boldsymbol{Q}} + \sum_{k=0}^{H_u-1} \left\| \boldsymbol{u}^k \right\|^2_{\boldsymbol{R}} + \left\| \begin{bmatrix} \theta^1_{EGR} \\ \theta^1_{VGT} \end{bmatrix} \right\|^2_{\boldsymbol{S}} \right) \tag{25}$$

subject to:

$$\begin{aligned} \boldsymbol{x}^{k+1} &= \boldsymbol{A}\boldsymbol{x}^k + \boldsymbol{B}\boldsymbol{u}^k \\ \boldsymbol{y}^k &= \boldsymbol{C}\boldsymbol{x}^k \\ \boldsymbol{u}_{lb} &\le \boldsymbol{u}^k \le \boldsymbol{u}_{ub} \\ \boldsymbol{x}_{lb} &\le \boldsymbol{x}^k \le \boldsymbol{x}_{ub} \\ \boldsymbol{x}^0 &= \boldsymbol{x}_{init} \\ k &= 0, 1, \ldots, H_p \end{aligned} \tag{26}$$

where H_p and H_u are prediction and control horizon length; $\boldsymbol{r}$ is the control reference; $\boldsymbol{Q}$, $\boldsymbol{R}$ and $\boldsymbol{S}$ are weight tuning parameters for reference tracking, control inputs and vavle positions; $\boldsymbol{u}_{lb}$, $\boldsymbol{u}_{ub}$, $\boldsymbol{x}_{lb}$, and $\boldsymbol{x}_{ub}$ are the lower bounds and upper bounds of inputs $\boldsymbol{u}$ and states $\boldsymbol{x}$; $\boldsymbol{x}_{init}$ is the latest measured value, the state feedback.

MPC will only apply the first solved control inputs $\boldsymbol{u}^0$ to the system. Then it will estimate parameters $\ln(c_1)$, c_2, c_3, and c_4 again, and reformulate the QP problem and get a new solution. This process is also known as receding horizon control.

For each cylinder, this MPC problem was formulated and solved independently. The solved θ_{SOI} was applied per cylinder, and the average of solved θ_{EGR} and θ_{VGT} were applied to the EGR and VGT valves.

4. EXPERIMENTAL SET-UP

The control plant is a six-cylinder heavy duty Scania D13 engine with specifications shown in Table 1. However, due to the sixth cylinder was malfunction during this paper work, only cylinder one to five were used in experiments. One 355 kW AC motor that worked as an engine motor and brake is used to control engine speed. The engine utilizes the cylinder pressure signal as feedback.

The control system is mainly based on National Instruments hardware. The hardware consists of a PXI chassis, Drivven-driver cards, and IO board. The PXI chassis has

Table 1. Engine specifications

Name	Value
Displaced volume	12.74 dm^3
Stroke	160 mm
Bore	130 mm
Connecting Rod	235 mm
Compression ratio	18:1
Number of Valves	4

an embedded controller that executed real-time software, and the FPGA board which is connected to the Drivven hardware and the embedded controller. The Drivven cards have power-drive modules to drive the throttles and injectors. The IO board receives the analog position signals and temperature signals. The control algorithm and user interface are running on a separate host PC with Windows 7 operating system. The control algorithm was programmed with Julia. The user interface was programmed by LabVIEW. The QP problem was solved by Interior Point Optimizer (IPOPT) (Wächter and Biegler, 2006). The PC communicates with the real-time system by TCP/IP and UDP network protocol. The in-cylinder pressure is measured by water-cooled Kistler 7061B pressure sensors and is sampled with the Leine-Linde crank angle encoder pulse every 0.2 crank angle degree. Inlet manifold and exhaust pressures are measured with Keller PAA-23S absolute pressure sensors. Intake and exhaust oxygen concentration are measured by Bosch LSU-4.9 oxygen sensors.

The fuel for the experiments was diesel, the mixture of 80 volume % Swedish 95 octane pump gasoline and 20 volume % n-heptane, and the mixture of 80 volume % pure ethanol and 20 volume % n-heptane. The n-heptane was added to avoid misfire since the cetane numbers of gasoline and ethanol are significantly smaller than diesel fuel. Another potential solution is the use of an intake air heater (Li et al., 2016).

5. EXPERIMENTAL RESULTS

Two fuel transition scenarios were conducted: the transition from diesel to gasoline/n-heptane mixture and the transition from gasoline/n-heptane mixture to ethanol/n-heptane mixture. Each transition takes approximately 30 to 40 minutes. The transition was done by turning off one fuel pipe and turning on the other fuel pipe. This is to simulate the situation that after running for some distance with one fuel, the user stops the car and fills the tank with another kind of fuel. The focus is on the gradual transition in the engine from one fuel to the newly added fuel, since many works had been done on the fuel steady situation.

5.1 Diesel to Gasoline/N-heptane Mixture

During this transition, the gross indicated mean effective pressure (IMEPg) was kept at 5 bar controlled by a proportional-integral (PI) controller. The engine speed was 1200 rpm.

Figure 2 shows the controller behavior at the beginning of diesel to gasoline/n-heptane transition. When the combustion timing θ_{CA50} target increased, the injection timing θ_{SOI} was retarded to track the reference. The ignition delay τ was mainly manipulated by valve position θ_{EGR} and θ_{VGT}. When the τ target increased, the VGT valve

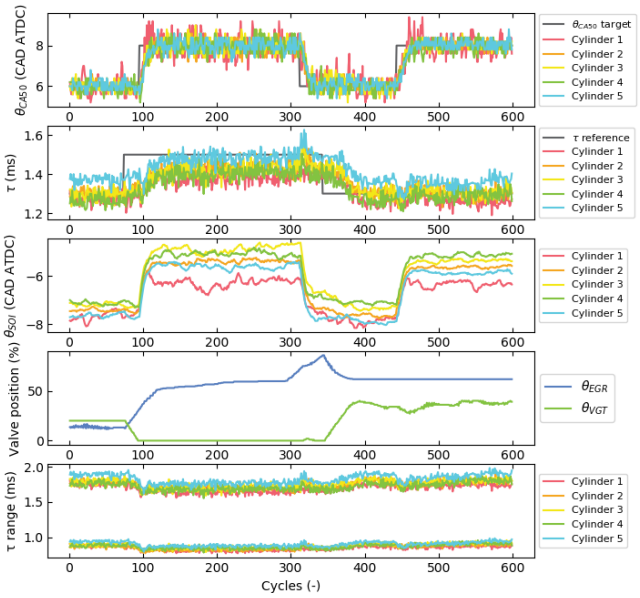

Fig. 2. Controller behavior at the start of diesel to gasoline/n-heptane transition. θ_{CA50} is the combustion timing, the CAD where 50% total heat are released; τ is the ignition delay; θ_{SOI} is the CAD of start of main injection; θ_{EGR} and θ_{VGT} are EGR and VGT valves opening. The same applies to Figs. 3-7

position θ_{VGT} was increased to raise the intake oxygen concentration and pressure, and the EGR valve position θ_{EGR} was decreased since the lower the EGR, the higher the intake oxygen concentration. The gas system dynamics was slower comparing with the injection system, and the tracking speed of ignition delay τ was slower than that of combustion timing θ_{CA50}.

When considering ignition delay τ, the control inputs (θ_{EGR}, θ_{VGT}) number were less than the control outputs (5 cylinder τ) number. This resulted in higher variance in τ than θ_{CA50}. In Fig. 2, the high cylinder to cylinder τ variation of cylinder 5 further degraded the τ control performance.

At cycle 100 to 300 in Fig. 2, the τ didn't achieve the set point. Noted that the θ_{EGR} was already 0 and θ_{VGT} was in a high position, which means current τ is the highest τ the controller could reach. The punishment term in cost function (25) stopped the θ_{EGR} from increasing further. This is because at this moment the engine fuel system was still the easy-ignited diesel.

The τ range calculated from estimated c_1, c_2, c_3, c_4 and (10) can reflect the change of fuel characteristics. The τ range is composed of the possible τ minimum, the (10) value in $O_{2\,IVC} = 24.00$ % and $p_{IVC} = 1.73$ bar which corresponds to $\theta_{EGR} = 0$ % and $\theta_{VGT} = 80$ %, and the possible τ maximum, the (10) value in $O_{2\,IVC} = 16.12$ % and $p_{IVC} = 1.06$ bar which corresponds to $\theta_{EGR} = 90$ % and $\theta_{VGT} = 0$ %. As we can see next, during the fuel transition, the possible τ range also varied in the same trend which served as an indicator for fuel properties.

Figure 3 shows the controller behavior in the middle of the transition, approximately 15 minutes after the fuel pipe

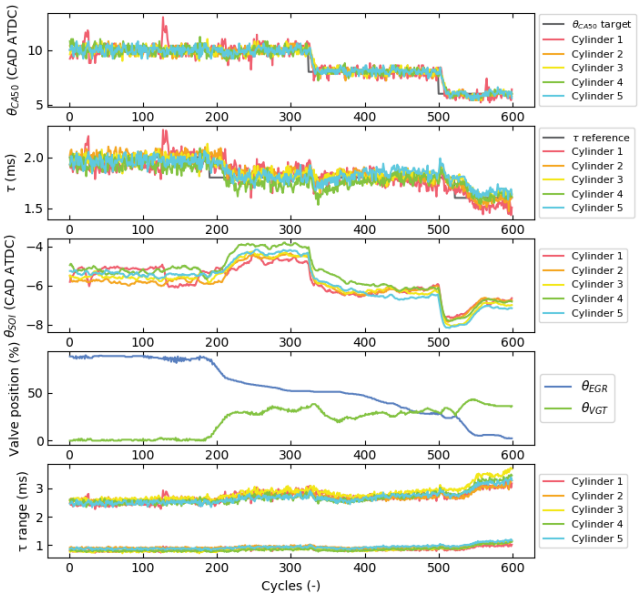

Fig. 3. Controller behavior in the middle of diesel to gasoline/n-heptane transition

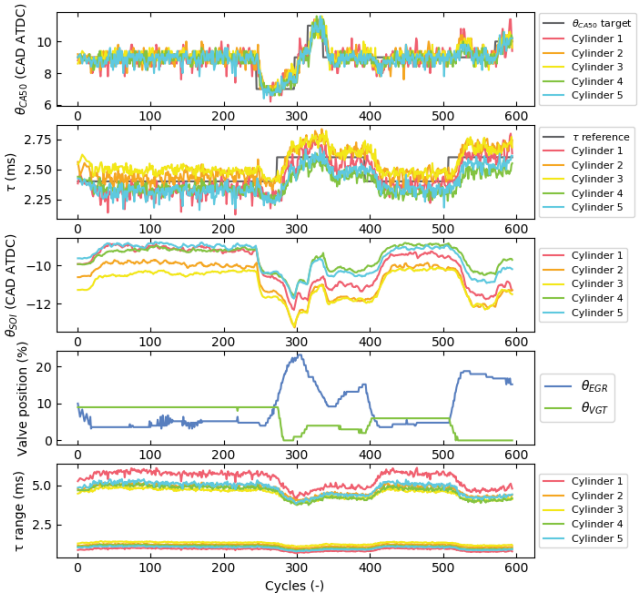

Fig. 4. Controller behavior in the end of diesel to gasoline/n-heptane transition

switch. Here the possible τ maximum is around 2.6 ms, bigger than that in Fig. 2, which is around 1.9 ms.

Figure 4 shows the controller behavior in the end of the transition, approximately 40 minutes after the fuel pipe switch. At this moment the possible τ maximum is around 5 ms. There is a clear difference in the τ range, especially the possible τ maximum. The more gasoline in the engine fuel system, the higher the possible τ maximum.

Figures 3 and 4 also show the adaptive MPC performance at different fuel transition stages. The performance is comparable with that in Fig. 2. But to keep the similar τ value, such as at the cycle 100 in Fig. 3 and the cycle 100 in Fig. 4, the actuators value θ_{EGR} and θ_{VGT} are totally different due to the fuel properties change.

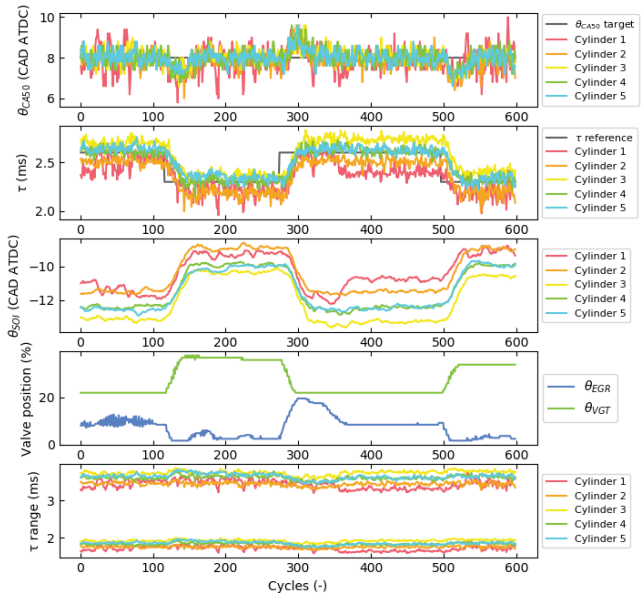

Fig. 5. τ transient, 6 minutes after the fuel pipe switch

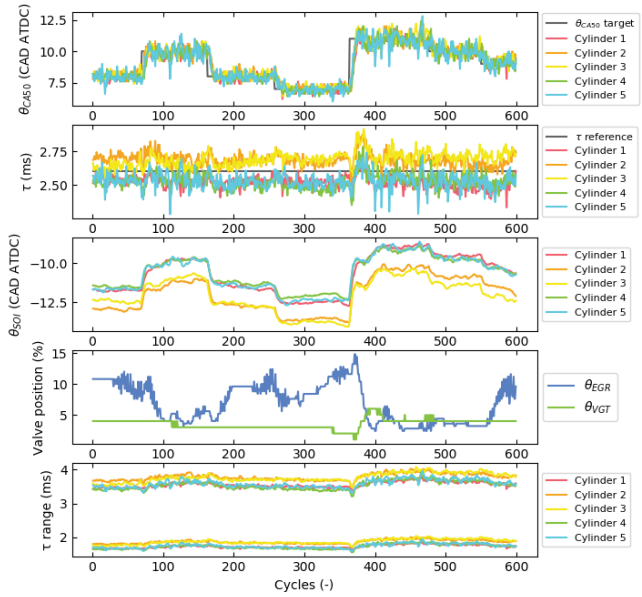

Fig. 6. θ_{CA50} transient, 16 minutes after the fuel pipe switch

5.2 Gasoline/N-heptane Mixture to Ethanol/N-heptane Mixture

During this transition, the IMEPg was still kept at 5 bar. Figures 5 and 6 show the τ reference transient and θ_{CA50} reference transient performance respectively at engine speed 1200 rpm. Figure 7 shows the performance in the engine speed N_{speed} transient scenario.

In the transition from gasoline/n-heptane mixture to ethanol/n-heptane mixture, The τ didn't change much. This is because gasoline and ethanol have similar cetane number and ignition properties. In this case, the τ range fails to be an indicator of the fuel transition process.

Observing from Fig. 2 to Fig. 7, the cylinder to cylinder ignition delay τ variations vary for different scenarios. This

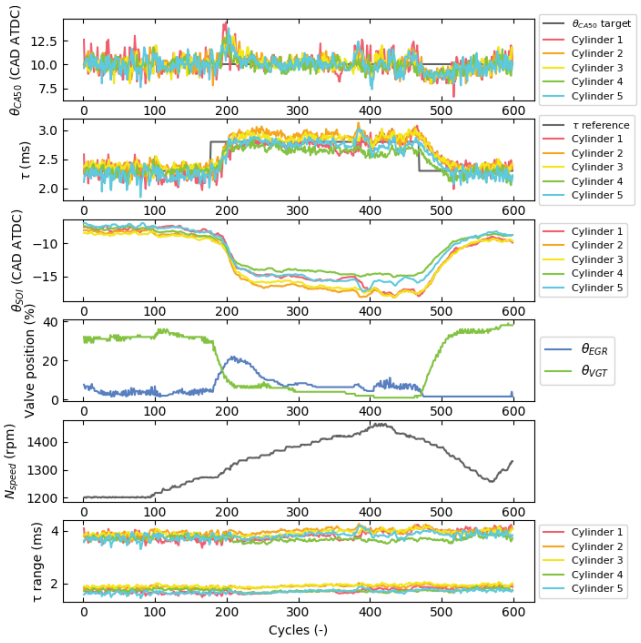

Fig. 7. N_{speed} transient, 25 minutes after the fuel pipe switch

might be another problem introduced by mutative fuel contents.

6. CONCLUSION

An adaptive MPC approach was proposed to control the flex-fuel multi-cylinder heavy duty CI engine. The controller was validated in the diesel to gasoline mixture transition and gasoline to ethanol mixture transition. The innovations in this work include: 1. Control of flex-fuel CI engine instead of the SI engine. 2. The fuel choice is not limited to two specific fuel species. 3. Fuel species is unknown in advance for the controller, which is not the case for nowadays flex-fuel controller.

ACKNOWLEDGEMENTS

The author would like to acknowledge the Competence Centre for the Combustion Processes, KCFP, and the Swedish Energy Agency for the financial support, Scania for supplying the experimental engine. The Chinese Scholarship Council is also thanked for the sponsorship of living expenses during the authors research. Rolf Johansson is a member of the eLLIIT Excellence Center at Lund University.

REFERENCES

Ahn, K.h., Yilmaz, H., Stefanopoulou, A., and Jiang, L. (2010). Ethanol content estimation in flex fuel direct injection engines using in-cylinder pressure measurements. In *SAE 2010 World Congress and Exhibition*, SAE Technical Paper 2010-01-0166. SAE International, Detroit, MI, USA, April, 2010.

Bengtsson, J., Strandh, P., Johansson, R., Tunestål, P., and Johansson, B. (2006). Model predictive control of homogeneous charge compression ignition (HCCI) engine dynamics. In *2006 IEEE Conference on Computer Aided Control System Design, 2006 IEEE International Conference on Control Applications, 2006 IEEE International Symposium on Intelligent Control*, 1675–1680. Munich, Germany, October, 2006.

Heywood, J.B. (2018). *Internal Combustion Engine Fundamentals*. McGraw-Hill Education, New York, United States.

Ingesson, G., Yin, L., Johansson, R., and Tunestål, P. (2015). Simultaneous control of combustion timing and ignition delay in multi-cylinder partially premixed combustion. *SAE International Journal of Engines*, 8(5), 2089–2098.

Johansson, R. (1993). *System Modeling and Identification*. Prentice-Hall, New Jersey, United States.

Kalman, R.E. (1960). A new approach to linear filtering and prediction problems. *Journal of Basic Engineering*, 82(1), 35–45.

Li, C. (2018). *Stratification and Combustion in the Transition from HCCI to PPC*. Ph.D. thesis, Department of Energy Sciences, Lund University, Lund, Sweden. ISBN: 9789177538707.

Li, C., Yin, L., Shamun, S., Tuner, M., Johansson, B., Solsjo, R., and Bai, X.S. (2016). Transition from HCCI to PPC: the sensitivity of combustion phasing to the intake temperature and the injection timing with and without EGR. In *SAE 2016 World Congress and Exhibition*, SAE Technical Paper 2016-01-0767. SAE International, Detroit, MI, United States, April, 2016.

Li, X., Yin, L., Tunestål, P., and Johansson, R. (2019). Learning based model predictive control of combustion timing in multi-cylinder partially premixed combustion engine. In *14th International Conference on Engines and Vehicles*, SAE Technical Paper 2019-24-0016. SAE International, Capri, Italy, September, 2019.

Maciejowski, J.M. (2002). *Predictive Control: with Constraints*. Pearson Education, Essex, England.

Mack, J.H., Aceves, S.M., and Dibble, R.W. (2009). Demonstrating direct use of wet ethanol in a homogeneous charge compression ignition (HCCI) engine. *Energy*, 34(6), 782–787.

Manente, V., Johansson, B., and Tunestål, P. (2009). Partially premixed combustion at high load using gasoline and ethanol, a comparison with diesel. In *SAE World Congress and Exhibition*, SAE Technical Paper 2009–01–0944. SAE International, Detroit, MI, USA, April, 2009.

Reitz, R.D. and Duraisamy, G. (2015). Review of high efficiency and clean reactivity controlled compression ignition (RCCI) combustion in internal combustion engines. *Progress in Energy and Combustion Science*, 46, 12–71.

Thring, R.H. (1989). Homogeneous-charge compression-ignition (HCCI) engines. In *1989 SAE International Fall Fuels and Lubricants Meeting and Exhibition*, SAE Technical Paper 892068. SAE International, Baltimore, Maryland, USA, September, 1989.

Wächter, A. and Biegler, L.T. (2006). On the implementation of an interior-point filter line-search algorithm for large-scale nonlinear programming. *Mathematical programming*, 106(1), 25–57.

Yin, L., Turesson, G., Tunestål, P., and Johansson, R. (2019). Evaluation and transient control of an advanced multi-cylinder engine based on partially premixed combustion. *Applied energy*, 233, 1015–1026.